Citation: A.Z. Panagiotopoulos, in M. Baus, L.R. Rull and J.P. Ryckaert, *Observation, prediction and simulation of phase transitions in complex fluids,* NATO ASI Series C, vol 460, pp. 463-501, Kluwer Academic Publishers, Dordrecht, The Netherlands (1995).

GIBBS ENSEMBLE TECHNIQUES

ATHANASSIOS Z. PANAGIOTOPOULOS
School of Chemical Engineering, Cornell University
Ithaca, NY 14853-5201 U.S.A.

1. Introduction

Phase transitions of real and model complex fluids are of significant scientific and technological interest. From a modeling point of view, it is often of considerable interest to predict, as accurately as possible, the phase behavior of a simplified system containing the essential interactions of interest. Computer simulations are a natural choice for this purpose, as they allow complete freedom in specification of the potential model. However, the prediction of the order and precise location of phase transitions from simulations is not a simple matter. Phase transitions are collective phenomena that occur over time and length scales that are not directly accessible by molecular dynamics or simple constant-volume Monte Carlo simulations. A range of specialized techniques developed in order to calculate the free energy and determine the behavior of systems at the vicinity of critical points are covered in the chapters by Binder and Frenkel. Many of these methods are relatively expensive from a computational point of view, requiring simulations for a series of state points or for a range of system sizes.

The focus of the present contribution is on a relatively simple and computationally inexpensive set of techniques known collectively under the (slightly misleading) name of "Gibbs ensemble" method [1]. While the Gibbs ensemble does not necessarily provide data of the highest possible accuracy and is not applicable to many important classes of systems, it is now commonly used for obtaining the phase behavior of fluids and mixtures. The main reason for this widespread use is probably the simplicity of the method. In particular, the method is easy to describe and program, and has an intuitive physical basis. It also places minimal demands on its user in terms of information on the approximate location of the phase diagram or other aspects of the behavior of a new system under study. For pure component systems, calculations of higher precision than are possible with the Gibbs ensemble technique can be performed by indirect calculation of the chemical potential for a series of state points [2] or thermodynamic-scaling Monte Carlo methods [3 ,4]. The Gibbs ensemble method is the technique of choice for determining the phase diagrams of fluid mixtures. The present chapter follows a series of reviews that the author has written in recent years, including a review of methodology and applications covering the period until 1991 [5] and a recent chapter in a NATO ASI

volume [6] focusing on applications of molecular simulation methods to high-pressure and supercritical systems. A degree of overlap of the present chapter with these earlier reviews is unavoidable. The present chapter is not an exhaustive review of applications of Gibbs ensemble techniques, but rather focuses on relatively recent calculations of the phase behavior of complex systems.

The plan of this chapter is as follows. We first present methodological aspects of Gibbs ensemble simulations, covering both elementary and advanced techniques. Issues related to approach to critical points and finite-size effects are covered in detail. Advanced techniques include configurational-bias sampling for chain molecules, biased particle transfers for ionic and associating fluids, methods to deal with reactive systems and specialized techniques for lattice systems. The Gibbs-Duhem integration method, although not strictly a "Gibbs ensemble" technique is also covered in the section on advanced techniques. Applications of the techniques to obtain information on phase transitions in simple fluids and mixtures are described next. These are followed by applications to polar fluids, including water, and applications to polar, associating and reacting fluids. The section on applications closes with a discussion of the phase behavior of both off- and on-lattice polymeric systems. We conclude this chapter by discussing the future outlook for molecular-based techniques for the determination of phase transitions in complex fluids.

2. The Gibbs ensemble

2.1. THEORETICAL FOUNDATIONS

Figure 1 illustrates the principle of the technique. Let us consider a macroscopic system with two phases coexisting at equilibrium. Gibbs ensemble simulations are performed in two microscopic regions within the bulk phases, away from the interface. Each region is simulated within standard periodic boundary conditions with images of itself. The thermodynamic requirements for phase coexistence are that each region should be in internal equilibrium, and that temperature, pressure and the chemical potentials of all components should be the same in the two regions. System temperature in Monte Carlo simulations is specified in advance. The remaining three conditions are respectively satisfied by performing three types of Monte Carlo "moves", displacements of particles within each region (to satisfy internal equilibrium), fluctuations in the volume of the two regions (to satisfy equality of pressures) and transfers of particles between regions (to satisfy equality of chemical potentials of all components).

The acceptance criteria for the Gibbs ensemble were originally derived from fluctuation theory [1]. An approximation was implicitly made in the derivation that resulted in a difference in the acceptance criterion for particle transfers proportional to $1/N$ relative to the exact expressions given subsequently [7]. A full development of the statistical mechanical definition of the ensemble was given by Smit *et al.* [8] and Smit and Frenkel [9]. We reproduce here the main lines of reasoning of Smit *et al.* [8] and Smit [10].

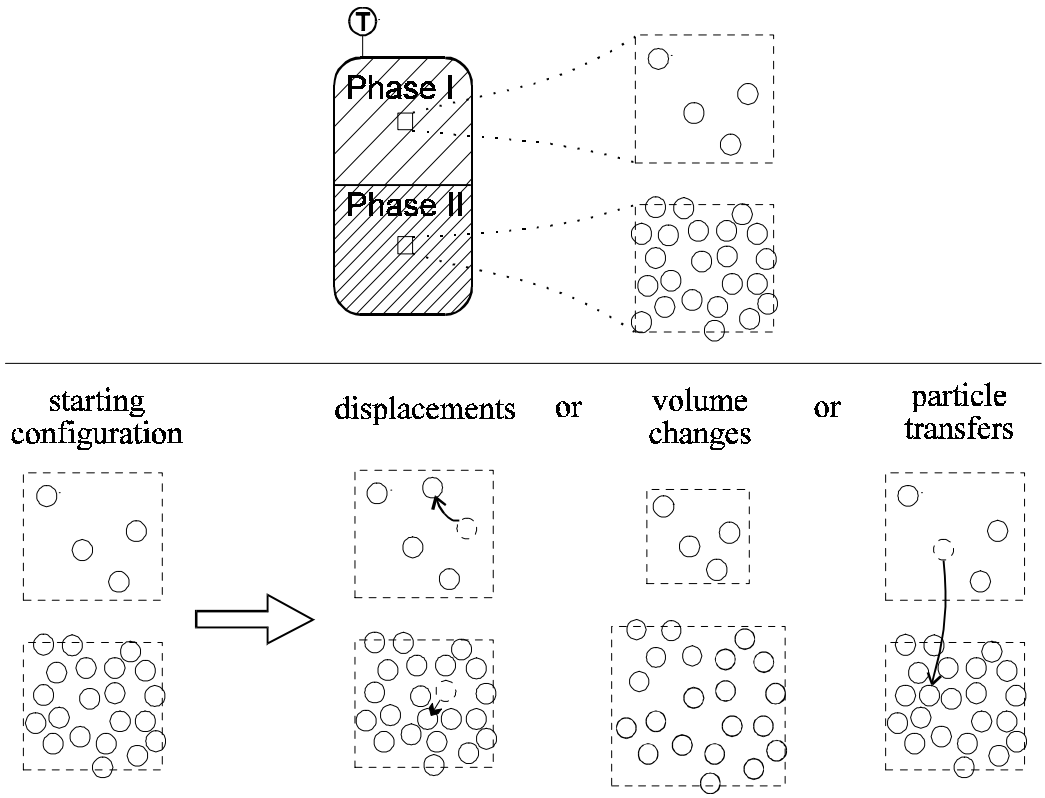

Figure 1. Schematic diagram of the Gibbs ensemble technique. A two-dimensional system is shown for simplicity. Dotted lines indicate periodic boundary conditions.

Let us consider a one-component system at constant temperature T, total volume V, and total number of particles N. The system is divided into two regions, with volumes V_I and V_{II} (= V–V_I) and number of particles N_I and N_{II} (=N–N_I). The partition function for this system, Q_{NVT}, is

$$Q_{NVT} = \frac{1}{\Lambda^{3N} N!} \sum_{N_I=0}^{N} \binom{N}{N_I} \int_0^V dV_I V_I^{N_I} V_{II}^{N_{II}} \int d\xi_I^{N_I} \exp\left[-\beta U_I(N_I)\right] \times \int d\xi_{II}^{N_{II}} \exp\left[-\beta U_{II}(N_{II})\right], \tag{1}$$

where Λ is the thermal de Broglie wavelength, $\beta=1/k_BT$, ξ_I and ξ_{II} are the scaled coordinates of the particles in the two regions and $U(N_I)$ is the total intermolecular potential of interaction of N_I particles. Equation 1 represents an ensemble with probability density, $\mathcal{P}(N_I, V_I; N, V, T)$ proportional to

$$\mathcal{P}(N_I, V_I; N, V, T) \propto \frac{N!}{N_I! N_{II}!} \exp\left(N_I \ln V_I + N_{II} \ln V_{II} - \beta U_I(N_I) - \beta U_{II}(N_{II})\right) \tag{2}$$

Smit *et al.* [8] used the partition function given by equation 1 and a free-energy minimization procedure to show that for a system with a first-order phase transition, the two regions in a Gibbs ensemble simulation are expected to reach the correct equilibrium densities.

The acceptance criteria for the three types of moves can be immediately obtained from equation 2. For a displacement step internal to one of the regions, the probability of acceptance is the same as for conventional constant-NVT simulations:

$$\mathcal{P}_{\text{move}} = \min\left[1, \exp(-\beta\Delta U)\right], \tag{3}$$

where ΔU is the configurational energy change resulting from the displacement. For a volume change step during which the volume of region I is increased by ΔV with a corresponding decrease of the volume of region II,

$$\mathcal{P}_{\text{volume}} = \min\left[1, \exp\left(-\beta\Delta U_I - \beta\Delta U_{II} + N_I \ln\frac{V_I + \Delta V}{V_I} + N_{II}\ln\frac{V_{II} - \Delta V}{V_{II}}\right)\right], \tag{4}$$

Equation 4 implies that sampling is performed uniformly in the volume itself. The actual implementation of such sampling is done by generating a uniformly distributed random number between 0 and 1, ξ, and obtaining ΔV as

$$\Delta V = \xi \times \delta v_{\max} \times \min(V_I, V_{II}) \tag{5}$$

where $\delta v_{\max}$ is the maximum fractional volume change allowed, a parameter adjusted to obtain the desired acceptance rate of the volume change steps. The acceptance criterion for particle transfers, written here for transfer from region II to region I is

$$\mathcal{P}_{\text{transfer}} = \min\left[1, \frac{N_{II}V_I}{(N_I + 1)V_{II}}\exp\left(-\beta\Delta U_I - \beta\Delta U_{II}\right)\right]. \tag{6}$$

Equation 6 can be readily generalized to multicomponent systems. The only difference is that the number of particles of species j in each of the two regions, $N_{I,j}$ and $N_{II,j}$ replace N_I and N_{II} respectively in equation 6. In simulations of multicomponent systems dilute in one component, it is possible that the number of particles of a species in one of the two regions becomes zero after a successful transfer out of that region. Equation 6 in this case is taken to imply that the probability of transfer out of an empty region is zero, which is also the mathematical limit of the probability of transfer, $\mathcal{P}_{\text{transfer}}$, as N_{II} is continuously reduced towards zero. In that case, as for all unsuccessful Monte Carlo steps, the old configuration is counted once more for the calculation of ensemble averages of any system property.

The acceptance rules to this point are for a simulation in which the total system is at constant number of molecules, temperature and volume. For pure component systems,

this is the only possibility because the phase rule requires that only one intensive variable (in this case system temperature) can be independently specified when two phases coexist. The vapor pressure is obtained from the simulation. By contrast, for multi-component systems pressure can be specified in advance, with the total system being considered at constant-*NPT*. The probability density for this case, $\mathcal{P}(N_I, V_I; N,P,T)$ is proportional to

$$\mathcal{P}(N_I, V_I; N, P, T) \propto \frac{N!}{N_I!\,N_{II}!} \exp\left(\begin{array}{r} N_I \ln V_I + N_{II} \ln V_{II} - \beta U_I(N_I) - \beta U_{II}(N_{II}) \\ -\beta P(V_I + V_{II}) \end{array} \right) \qquad (7)$$

and the only change necessary in the algorithm is that the volume changes in the two regions are now made independently. The acceptance criterion for a volume change step in which the volume of region I is changed by ΔV_I and the volume of region II by ΔV_{II} is then

$$\mathcal{P}_{\text{volume}} = \min\left[1, \exp\left(\begin{array}{r} -\beta\Delta U_I - \beta\Delta U_{II} + N_I \ln \frac{V_I + \Delta V_I}{V_I} + N_{II} \ln \frac{V_{II} - \Delta V_{II}}{V_{II}} \\ -\beta P(\Delta V_I + \Delta V_{II}) \end{array} \right)\right]. \qquad (8)$$

A simple variation of the basic methodology is the particle identity exchange algorithm [11], appropriate for the study of mixtures of components that differ greatly in molecular size. The technique is illustrated schematically in Figure 2. Let us consider a binary mixture with components A and B, and designate the component with the larger size as component B. In the particle identity exchange algorithm, only component A is transferred directly between regions in the Gibbs ensemble simulation. Component B is transferred indirectly, by changing a particle of type A into one of type B in one of the two regions with a simultaneous reverse change in the other region. The move is accepted with a probability (written here for a change of A into B in region II),

$$\mathcal{P}_{\text{exchange}} = \min\left[1, \frac{N_{II}^A N_I^B}{(N_I^A + 1)(N_{II}^B + 1)} \exp\left(-\beta\Delta U_I - \beta\Delta U_{II}\right)\right]. \qquad (9)$$

The conditions between the chemical potentials of the two components in the two regions satisfied by these two sets of moves are then

$$\begin{array}{rl} \mu_I^A = \mu_{II}^A & (\text{from transfer step}) \\ \mu_I^B - \mu_I^A = \mu_{II}^B - \mu_{II}^A & (\text{from exchange step}). \end{array} \qquad (10)$$

which are sufficient to ensure the equality of the chemical potentials of both components in the two phases. The method is easily generalized for systems with more than two components.

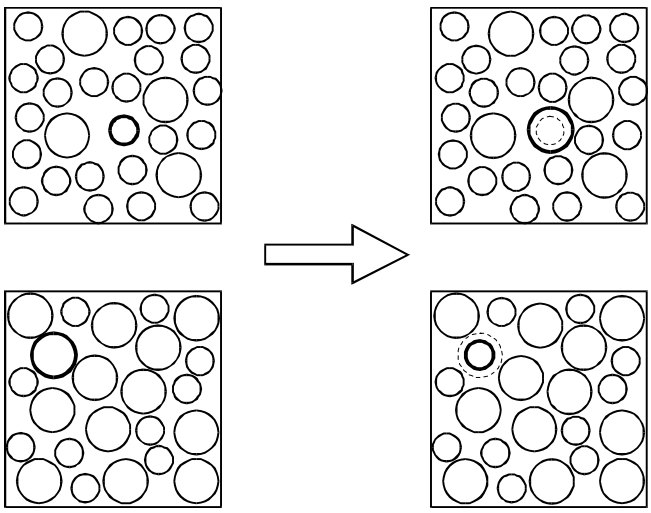

Figure 2. Schematic illustration of a particle identity change algorithm.

Simulations of phase equilibria in the Gibbs ensemble do not require prior knowledge or calculation of the chemical potentials of components in a system. However, it is a useful test of the convergence of simulations to ensure that the values of the chemical potentials in the liquid and gas phases are equal. During the particle transfer steps, the change in configurational energy of a region that would have resulted by addition of a particle is clearly related to the "test particle" energies, U^+, used in the Widom equation for calculation of chemical potentials in constant-NVT simulations:

$$\mu_i = -kT \ln \left\langle \exp\left(-\beta \Delta U^+\right) \right\rangle + kT \ln \rho_i, \tag{11}$$

where μ_i is the chemical potential of component i and ρ_i is the density of component i ($\rho_i = N_i / V$). Smit and Frenkel [9] have obtained a similar expression valid for Gibbs ensemble simulations, written here for region I:

$$\mu_i = -kT \ln \left\langle \frac{V_I}{N_{I,1}+1} \exp\left(-\beta \Delta U_1^+\right) \right\rangle, \tag{12}$$

where U_1^+ is the configurational energy change of region I during attempted transfers of particles of species i. The difference between the two expressions is that equation 12 takes into account fluctuations in volume and number of particles in the regions of a Gibbs ensemble simulation. The calculated values of the chemical potentials from equations 11 and 12 typically differ less than simulation uncertainty [9], except when very few particles are present in one of the two regions.

2.2. Approaching Critical Points and Finite-Size Effects

Approaching critical points by simulations is complicated by the use of a finite system and periodic boundary conditions. At any critical point, a characteristic correlation length for the macroscopic thermodynamic system approaches infinity. This divergence cannot be captured by simulations, which constrain fluctuations to the box length used. In the following paragraphs, we restrict our attention to the question of how the location of critical points can be predicted from Gibbs ensemble simulations.

When the system is away from the critical point of the phase transition under study (as for example in figure 3), the equilibrium densities and compositions of the coexisting phases can be simply determined by averaging the observations after equilibration. A first sign of the approach to a critical point is the occasional appearance of "abnormal" fluctuations in the properties of the two regions that are caused by transient formation of droplets or bubbles of the "wrong" phase in one of the two boxes. The presence of "drifts" in the properties of the coexisting phases has been pointed out by Smit [12 ,10]. Since it is not clear in general what should be taken to constitute an "abnormal" fluctuation or "drift", it is best to establish an objective way to extract information on equilibrium compositions from such a run. One such way is to generate histograms of the frequency of occurrence of a certain density in each of the two regions. The equilibrium densities can be defined as the densities corresponding to the peaks of the probability distribution function. "Drifts" of the densities of the two regions tend to appear as areas outside the main peaks, and have no significant effect on the location of the maxima of the density probability function.

As one approaches a critical point even closer, the situation becomes even more problematic. The driving force for a Gibbs ensemble simulation to remain in a state with two stable regions of different density is the free energy penalty for formation of interfaces within each of the two regions. When the system is close to a critical point, the penalty for formation of interfaces is small, and there are frequent exchanges of the identity of the two boxes as shown in figure 4. In such cases, the only way to obtain estimates of the coexisting densities is to obtain the density probability function (figure 5). The density probability function is quite noisy, and the coexisting densities cannot be determined to high accuracy. Statistical uncertainties of the coexistence densities can be obtained by constructing separate histograms for smaller segments of the run.

At even higher temperatures above the critical point, the two-peaked structure of the density distribution function disappears, and a broad distribution with a single peak is observed. It should be pointed out that a Gibbs ensemble simulation at conditions for which the state of lowest free energy for the system is a single homogeneous phase is inherently unstable with respect to the particle numbers and volumes of the two regions. As long as the average density in the two regions is the same, the conditions of equality of pressure and chemical potentials between them are satisfied. Thus, the extents of the two regions tend to drift and sooner or later one of the two disappears. It should be understood in such cases that the Gibbs ensemble simulation has not "failed," but rather has converged to a single-phase solution.

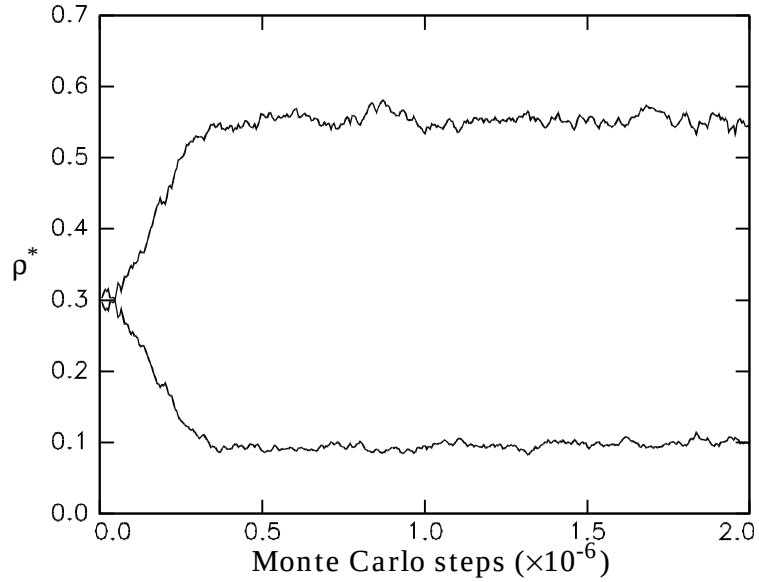

Figure 3. Reduced density, ρ^*, versus the number of Monte Carlo steps for a Gibbs ensemble simulation of a system of 1800 Lennard-Jones particles in three dimensions at $T^* = 1.20$, initially in two regions of equal volume and density.

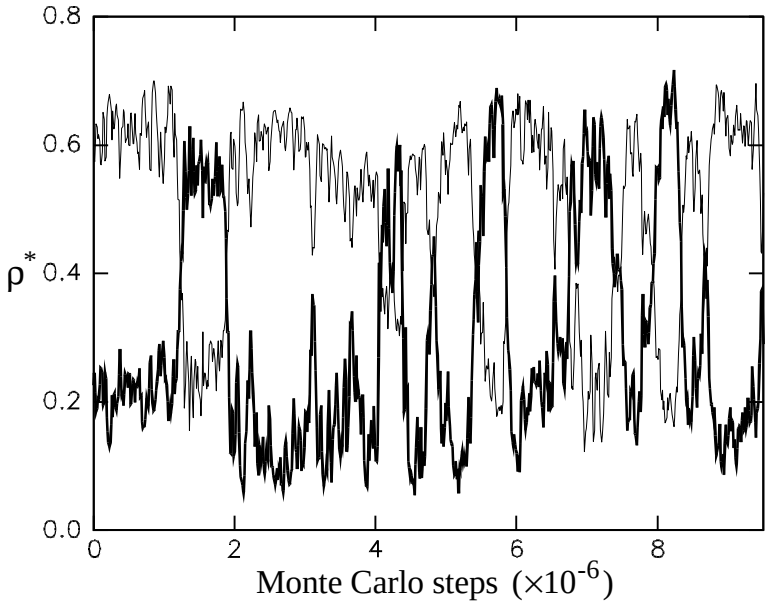

Figure 4. Reduced density, ρ^*, versus number of Monte Carlo steps for a Gibbs ensemble simulation of a system of 205 Lennard-Jones particles in two dimensions at $T^* = 0.50$. The potential is cut off at a distance of 2.5σ.

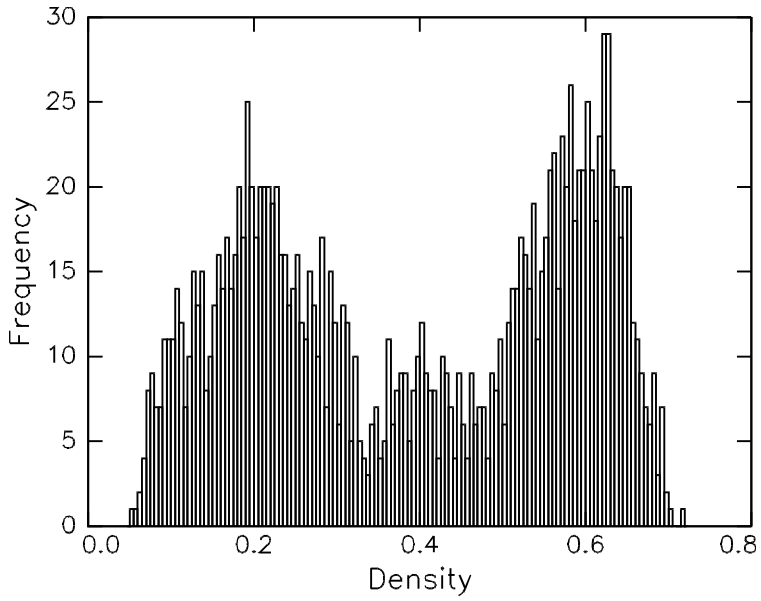

Figure 5. Density probability function for the simulation of figure 4.

Simple thermodynamic models that do not incorporate the effects of fluctuations predict that the coexistence curve for two-phase equilibria has the "classical" parabolic shape, independent of the dimensionality of the system, while experimental results and modern theories of critical phenomena indicate that the shape of coexistence curves are flatter close to critical points, with a characteristic exponent β taking the value 1/8 in two dimensions and approx. 1/3 in three. In principle, Gibbs ensemble simulations, as all simulations performed on a finite system, cannot capture the divergence of the correlation length that characterizes critical points and gives rise to the non-classical values for critical exponents. However, contrary to simple mean-field theories, all fluctuations with correlation lengths that fit within the simulation box are taken into account. We therefore expect, in principle, Gibbs ensemble simulations to fall somewhere between mean-field theories and experimental data with respect to the behavior of the phase envelope close to critical points.

In many simulation studies using the Gibbs ensemble, the rectilinear diameter rule and the scaling relationship for the width of the coexistence curve are used to estimate the location of the critical point.

$$\begin{aligned} \frac{\rho_L + \rho_G}{2} &= \rho_c + C(T_c - T) \\ \rho_L - \rho_G &\propto (T_c - T)^{\beta} \end{aligned}, \qquad (13)$$

where β is an exponent taken to be equal to its non-classical value ($\beta \approx 0.325$) in three dimensions and 1/8 in two.

The shape of the coexistence curve obtained from Gibbs ensemble simulations at the vicinity of the critical point has been examined in detail by Mon and Binder [13] for the two-dimensional lattice-based Ising model, by Recht and Panagiotopoulos [14] for a continuous-space square-well binary mixture in two and three dimensions and by Panagiotopoulos [15] for truncated Lennard-Jones potentials in two and three dimensions. In two dimensions, a cross-over in the shape of the coexistence curve from an apparent non-classical exponent away from the critical point to a classical value at the vicinity of the critical point was observed in both lattice and off-lattice simulations. This behavior is illustrated in figure 6, which refers to a two-dimensional Lennard-Jones fluid. Close to the critical temperature, the width of the coexistence curve follows a mean-field exponent (β=1/2), rather than the non-classical value of 1/8. This occurs for the following reason. Away from the critical region the correlation length is considerably less than L, so that the simulation can accommodate the proper fluctuations in density and the system shows the non-classical behavior, β=1/8. Very near the critical point, however, the correlation length exceeds L; the system cannot accommodate the long-range fluctuations, and classical behavior, β=1/2, is observed. By contrast, for the three-dimensional systems, the non-classical apparent value of the exponent persists for a wide range of temperatures, up to the immediate vicinity of the critical point. This difference between the behavior of the two-dimensional and three-dimensional systems is probably due to the larger importance of the truncation of fluctuations for the two-dimensional systems. In two dimensions the correlation length grows more rapidly than in three as the critical temperature is approached (the correlation length exponent ν=1 for two dimensions and ν=0.63 for three).

In practical terms, care certainly seems justified in extrapolating phase coexistence data from Gibbs ensemble simulations to the critical point, especially for two-dimensional systems. When data away from the critical point that do not show finite-size rounding are used to estimate the critical parameters, good agreement is obtained with calculations of critical temperatures that are based on block density distribution techniques (section 3.1.1). There is no guarantee, however, that data away from the critical point will follow the limiting scaling laws. When performing Gibbs ensemble simulations close to critical points, especially if the aim is to estimate critical exponents, one is always between the Scylla of finite-size rounding and the Charybdis of being too far from the critical point for the limiting critical behavior to emerge. An additional factor to consider is control of linear system size, which is essential for the accurate determination of critical parameters. Because system size of each of the two regions has to vary in Gibbs ensemble simulations, control of system size can only be performed in an average sense, and trial-and-error calculations are often required.

Although the discussion above is based on observations using Gibbs ensemble simulations, similar findings on the shape of the coexistence curve for the three-dimensional Lennard-Jones potential have been recently reported [16] when an accurate thermodynamic-scaling Monte Carlo method is used to obtain the coexistence curve at the vicinity of the critical point.

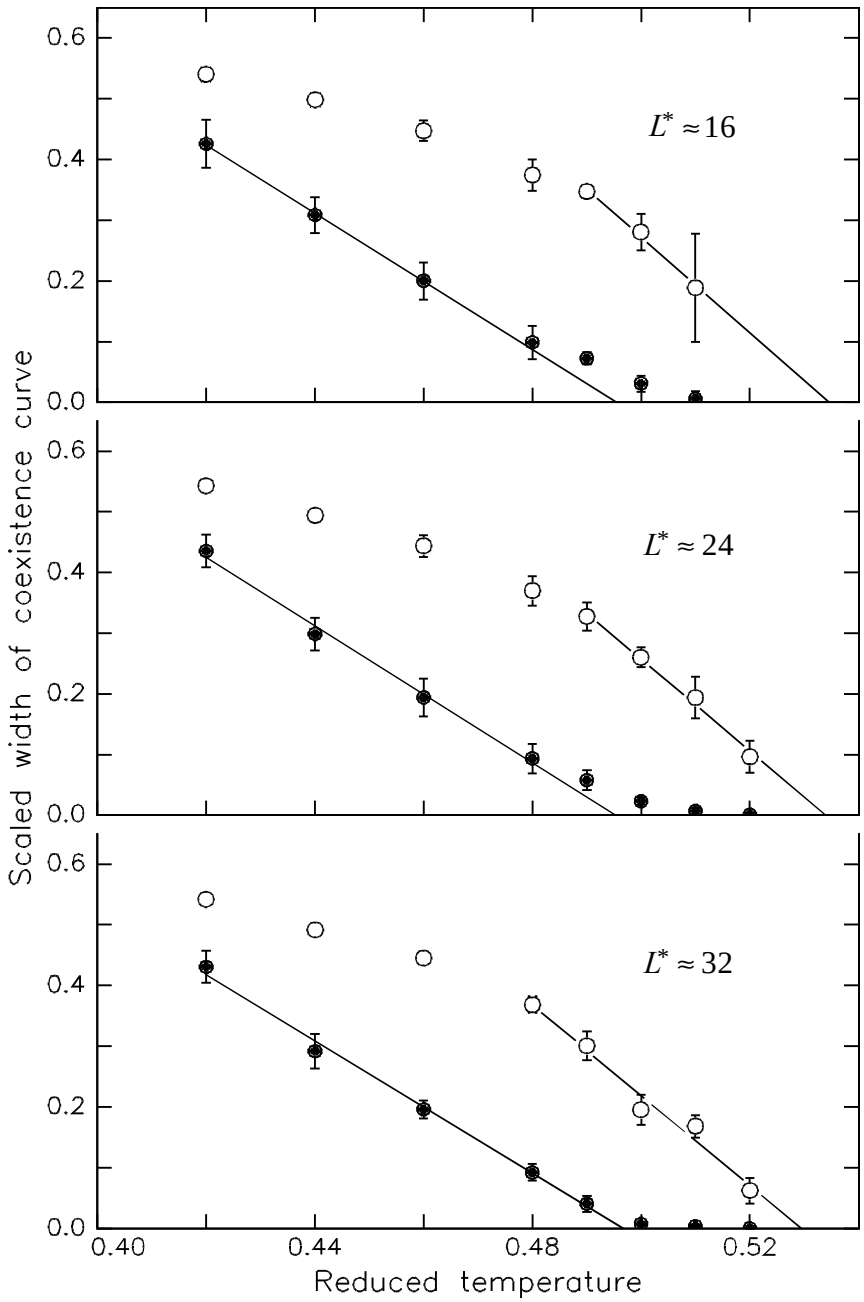

Figure 6. Scaled width of the coexistence curves versus reduced temperature for two-dimensional systems with $r_c^* = 5$ and $L^* \approx 16, 24$ and 32. (●) $(\rho_L^* - \rho_G^*)^2$; (○) $5 \times (\rho_L^* - \rho_G^*)^8$. The lines are linear least-squares fits of the corresponding data points. Adapted from [15].

2.3. VARIATIONS ON THE CENTRAL THEME

An important area of potential application of Gibbs ensemble simulations is in the study of equilibria for confined fluids. The necessary methodological developments have been presented in [17]. For confined fluids, two primary types of equilibria can be described. The first is adsorption equilibrium between a bulk (free) fluid phase and the interior of an adsorbing material. Real adsorbents (such as activated carbon) have complex, often poorly characterized interior geometries. However, studies of adsorption are often performed for the idealized geometries of a slit or a cylindrical pore. The equilibrium constraints are that chemical potentials of all components in the bulk and in the interior of pore should be the same. There is no requirement for mechanical equilibrium. This implies that no volume change step is necessary for Gibbs simulations, only displacement and particle transfer steps. Gibbs ensemble simulations of adsorption are almost identical to grand canonical simulations, the only difference being that the total composition of the system is imposed, rather than the chemical potentials in the exterior of the pore.

The second type of equilibria that are important for confined fluids are capillary condensation phenomena, which involve coexistence of two phases in the interior of a pore. Application of the Gibbs method for these systems requires internal, mechanical and chemical potential equality, just as for the case of bulk fluids. Mechanical equilibrium is achieved by changes in *length* (for the case of cylindrical geometry) or *area* (for the case of slits).

An alternative technique for determining equilibria for confined fluids is direct simulation of a two-phase system [18], which is possible because the adsorbing walls act as nucleation sites. Larger systems, and therefore longer simulations, are required for direct two-phase simulations, because of the presence of interfaces, but two-phase simulations have the advantage that they can provide information on the dynamics of the phase transition and the structure of the interfacial region.

A simple modification for the study of membrane equilibria in fluid mixtures has been proposed in [7]. The modification involves imposing the condition of chemical potential equality only for components that are membrane-permeable. A similar technique can be used for other systems for which some components are not found in one of the coexisting phases. Examples of such systems are equilibria involving sorption of small molecules in polymers and vapor-liquid equilibria in electrolyte solutions for which the concentration of electrolyte in the gas phase is negligible [19].

2.4. ADVANCED TECHNIQUES

2.4.1. Configurational-bias Sampling and the Gibbs Ensemble

For multisegment molecules (for example a unified-atom model of an *n*-alkane), the simple particle transfer move of the Gibbs ensemble becomes impractical because of steric overlaps. A large improvement in sampling efficiency for such systems results from combination of configurational-bias methods with the Gibbs ensemble, as suggested by Mooij *et al.* [20] and, independently, Laso *et al.* [21]. Configurational-bias methods are

discussed in the chapter by Frenkel. In this chapter we only outline the aspects of configurational-bias sampling applied to the Gibbs ensemble.

Consider a Gibbs-ensemble simulation of a system with multisegment particles. For simplicity, we assume that all particles have the same number of segments l. Now consider a trial particle transfer move from region II to region I. First, the particle to be transferred is inserted, in a segment-by-segment fashion, into region I. For the first segment, the insertion takes place in a random position, and the weighting factor, $w_I(1)$ calculated from

$$w_I(1) = \exp\left[-\beta U_{I,1}\right] \tag{14}$$

where $U_{I,1}$ is the energy of interaction of the added segment with the rest of the particles in region I. The next insertion, of segment 2, is performed by selecting m trial directions for growth, and choosing one of them, say the k-th, with probability

$$\mathcal{P}_k = \frac{\exp\left(-\beta U_{I,2}^k\right)}{w_I(2)} \tag{15}$$

where $\mathcal{P}_k$ is the probability of selecting growth direction k, $U_{I,2}^k$ is the energy of interaction of the added second segment in growth direction k with the rest of the system, and $w_I(2)$ is given by

$$w_I(2) = \sum_{i=1}^{m} \exp\left(-\beta U_{I,2}^i\right) \tag{16}$$

The same procedure is repeated for the third, fourth and so on segments, until segment l has been inserted. At that point, the total Rosenbluth weight in region I is calculated

$$W_I = \prod_{j=1}^{l} w_I(j) \tag{17}$$

Note that, in the case m=1 for all segments, the procedure is fully equivalent to random (Widom-type) insertions. The total Rosenbluth weight, W_I is then simply the total energy of interaction of the inserted molecule with the rest of the system.

A similar procedure is followed for removal of the molecule to be transferred from region II. An important detail pointed out by Mooij *et al.* [20], is that the *same set* of trial directions should be used in considering segment-by-segment removal as the ones used in segment-by-segment additions, with one of the directions constrained to be the actual direction along which the segment being removed is located. The Rosenbluth weight, W_{II} of the molecule in region II is calculated in a manner analogous to equation

(17). Acceptance of the particle transfer moves then takes place with probability directly similar to that of equation (6), modified with the Rosenbluth weights

$$\wp_{\text{transfer}} = \min\left[1, \frac{N_{II}V_I W_I}{(N_I+1)V_{II}W_{II}}\right]. \tag{18}$$

The different appearance of equation (18) versus equation (6) is due to the incorporation of the energy differences into the Rosenbluth weights. It can be shown [20] that when the acceptance criterion of equation (18) is used, the particle transfer scheme described above satisfies the detailed balance condition.

For computational efficiency [22] it is advisable to use an increasing number of trial directions as one proceeds along a chain, so that the computational effort that has been "invested" in early stages of a given attempted insertion not be wasted because only a limited number of growth directions is tested at later stages.

Cracknell *et al.* [23] have described a rotational insertion bias method for the Gibbs ensemble applicable to dense phases of structured particles (e.g. water). The method is a special case of the configurational-bias technique described above. The rotational insertion bias method consists of selecting a random location in the phase into which a particle is being transferred, and calculating the Boltzmann factors and Rosenbluth weights for several possible orientations of the molecule to be inserted. This corresponds to a single growth step in the configurational-bias method of Laso *et al.* [21] and Mooij *et al.* [20].

2.4.2. Biased particle transfers for ionic and associating fluids

A problem somewhat related to the one described in the previous paragraph for insertions of chain molecules or structured particles is encountered in simulations of strongly interacting associating and ionic fluids. For example, for ionic fluids, at low reduced temperatures for which phase separation is observed, the low-density phase consists almost exclusively of clusters of ions, the dominant species being typically ion pairs. It is clear that attempted transfers into or out of such a clustered system need to take into account the presence of clusters in order to lead to a reasonable probability of acceptance of the transfer moves.

The problem of biased pair insertions and removals in ionic systems has been addressed by Orkoulas and Panagiotopoulos [24]. For random (unbiased) insertions, the probability density of inserting a counterion a distance r from a randomly placed ion is

$$W_0(r) = \frac{1}{L^3} 4\pi r^2 \qquad\qquad r < \frac{L}{2} \tag{19}$$

For distances greater than L/2, the spherical shell expands outside the simulation cube and the probability density $W_0(r)$ is defined by the intersections of the spherical shell with the cube. The derivation for this case in complicated and can be found elsewhere [25]. $W_0(r)$ is a decreasing function of r and eventually reaches zero for a distance

of $\sqrt{3}\cdot L/2$. Orkoulas and Panagiotopoulos [24] propose preferentially sampling distances close to contact on insertions, using a biasing function such as

$$W(r) = \frac{1}{C}\exp(-\alpha r) \qquad \text{for} \qquad \sigma \le r \le \frac{\sqrt{3}L}{2} \tag{20}$$

where L is the simulation box edge, α is an adjustable parameter governing the steepness of the biasing function and C is a normalization constant to satisfy the condition that the integral over the simulation box of W(r) be unity. For the reverse step of pair removals, the unbiased (random) probability of selecting a given counterion is simply

$$P_0(i) = 1/N_c \tag{21}$$

To bias selection of counterions towards bonded-pair neighbors, a modified probability of selection is used:

$$P(i) = \frac{W(r_i)}{\sum_{j=1}^{N_c} W(r_j)} \tag{22}$$

where $W(r_i)$ is the biasing function of equation (20). With this particular mechanism for selecting the counterion to be removed and the position of the one to be inserted, the acceptance probability of the particle transfer step (equation 6) written for a pair transfer from region II to region I becomes

$$\mathcal{P}_{\text{transfer}} = \min\left[1, \frac{W_I(r)P_{0,II}(i)}{W_{0,I}(r)\ P_{II}(i)}\exp\left(-\beta\Delta U_I - \beta\Delta U_{II} - \ln\frac{(N_I+1)^2\,V_{II}}{N_{II}^2\,V_I}\right)\right]. \tag{23}$$

where we have assumed that a distance r between counterions in region I was selected in the insertion step, and that counterion i in region II was selected in the removal step. N_I and N_{II} are the total number of ions or counterions (so that there are $2N_I$ total ions in region *I*). The reason the numbers appear squared in the right-hand side of equation 23 is that the transfer step now involves two particles simultaneously.

Distance-biasing is an appropriate technique for ionic systems which contain a potential term that strongly favors short interionic distance. For the general case of associating fluids, Tsangaris and de Pablo [26] have proposed a biasing scheme which can be used to facilitate canonical-ensemble and Gibbs-ensemble simulations in strongly associating systems. In the method of Tsangaris and de Pablo, a bonding region is defined around a particle that contains an association site, and the balance of volume is considered "non-bonding". Another particle that also carries an association site experiences strong interactions within these regions, but the relative volume of the regions is small, which renders equilibration quite difficult. By introducing a bias so that

(on particle insertions) the bonding regions are preferentially sampled over the non-bonding ones, equilibration is greatly facilitated. Removal of the bias is achieved in a way similar to that used in equation 23.

2.4.3. Reactive Fluids

Chemical reactions can be considered as an extreme case of association. Shaw [27] introduced an ensemble in which the number of atoms, rather than the number of molecules is kept constant during the simulation and applied it to the relatively simple case of a reaction that conserves the number of molecules. More recently, Johnson *et al.* [28] and Smith and Triska [29] independently developed a generalized framework for handling chemical reactions in canonical or Gibbs-ensemble simulations. The technique is illustrated schematically in figure 7 for the case of a simple reaction A+B↔C. For simplicity, the canonical version of the algorithm is illustrated. The forward reaction step involves replacing one randomly selected particle of species A and one randomly selected particle of species B with a particle of species C. In principle, any position of the newly created particle C is acceptable. However, in order to increase the probability of acceptance of the move, the particle is placed with its center coinciding with the center of the destroyed particle B. It is clear that such a choice would be optimal if the size of components B and C is comparable. The forward reaction step is accepted with probability proportional to

$$\mathcal{P}_{\rightarrow} = \min\left[1, \frac{K(T)}{V}\frac{N_A N_B}{N_C + 1}\exp(-\beta\Delta U)\right] \tag{24}$$

where $K(T)$ is the ideal-gas equilibrium constant, $K(T) = \exp(-\Delta G^0 / kT)$. It is interesting to note that in equation 24 the term $K(T)/V$ plays a role similar to that of a "biasing" function to drive the reaction forward. For the reverse reaction step, the acceptance criterion is, similarly,

$$\mathcal{P}_{\leftarrow} = \min\left[1, \frac{N_C}{(N_A + 1)\ (N_B + 1)}\frac{V}{K(T)}\exp(-\beta\Delta U)\right] \tag{25}$$

In order to satisfy the detailed balance condition on the reverse reaction step, a particle of species B takes the place of the particle of species C that is eliminated, and a particle of species A is placed in a random position within the simulation cell.

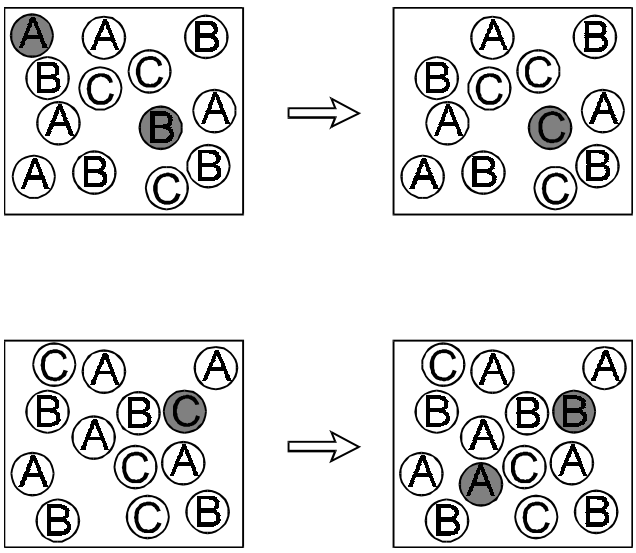

Figure 7. Schematic illustration of the forward (upper half) and reverse (lower half) reaction steps for a three-component system in which the reaction A+B↔C takes place.

2.4.4. Lattice Gibbs Ensemble Simulations

Lattice models have a long history in statistical mechanics, especially of polymeric fluids. An example of such a model is the simple lattice polymeric model that Flory used as the underlying "picture" for deriving his expression for the free energy of a polymeric system. The three-dimensional version of the model is on the simple cubic lattice with coordination number 6, while the two-dimensional version is on the simple square lattice with coordination number 4. Simulations on lattice models are typically less computational demanding than comparable continuous-space models for equivalent system sizes, thus permitting the study of phenomena of intrinsically longer time scales.

Somewhat counter-intuitively, the determination of the phase behavior of continuous-space chain models has proceeded at a faster pace than for lattice models. Direct interfacial simulations have been used by Madden *et al*. [30] to determine the phase diagram for chains of length 100 on the simple cubic lattice. While this method gives direct determination of phase coexistence it nevertheless suffers from the disadvantages that the interphase constitutes a significant part of the simulated system, and that it is difficult to obtain information on the properties of the dilute (gas) phases except in the immediate vicinity of the critical point. Sariban and Binder [31] and Deutsch and Binder [32] have studied coexistence in symmetric binary polymer blends. The Monte Carlo technique used takes advantage of the symmetry of the system to enable determination of the phase boundary. Histogram techniques have recently been used to obtain the phase behavior at the vicinity of critical points for asymmetric polymer blends [33] and to study demixing in mixtures of stiff and flexible polymers

[34]. These techniques are highly successful in the study of systems at the vicinity of critical points and are described in detail in the chapter by Binder in this volume.

The main difficulty in applying the Gibbs ensemble to lattice models is the difficulty in changing the volume of a lattice. The only way that periodic boundary conditions can be maintained on change in volume of a lattice is when the change involves addition or removal of a complete lattice layer. Such changes represent significant perturbations to the system, and have very small probabilities of acceptance at typical liquid densities. Polymer connectivity complicates this situation even more.

Mackie *et al.* [35] have recently developed a method for performing constant-pressure simulations on lattice models that can be easily extended to the Gibbs ensemble [36]. The method allows for the expansion or contraction of a lattice of chain molecules by cutting and regrowing any chain that crosses the plane that is to be added or removed. The method is shown schematically in figure 8 for the simple square lattice, but generalization to different dimensionalities and other lattice structures is simple.

For a lattice removal step, a plane of the lattice to be removed (shaded layer in the upper part of figure 8) is first selected with uniform probability. Then the polymer chains with beads on this layer are marked, and one of the two ends of the chain is selected with equal probability to be eliminated. The beads of the marked chains are then removed one at a time starting from the cut end and ending at the point at which a single uncut chain fragment remains. The Rosenbluth weight [37] of the old configuration is calculated during this removal step in a procedure analogous to that described by equations 14-17. Then the selected layer is removed, and the chains are regrown to their original dimensions. Chains that have been completely removed from the system because their end was found in the removed layer are inserted at random positions. The total Rosenbluth weight of the new configuration, W_{new} is computed as the product of the Rosenbluth weights of the chains that have been partly or completely regrown. The move is accepted with probability

$$P_{acc} = \min\left[1, \frac{W_{new}}{W_{old}} \exp\left(-\beta\Delta U + N \ln \frac{V+\Delta V}{V} - \beta P \Delta V\right)\right]. \tag{26}$$

The lattice expansion step proceeds as shown in the lower half of figure 8. A plane between two layers of the lattice is selected with uniform probability. The polymer chains that are cut by this plane are marked, and one of the two ends is selected with equal probability. Then beads of the marked chains are removed with a procedure analogous to that used in the layer removal step. In order to satisfy the detailed balance condition, it is necessary to select a number of chains at random to insert with one end located in the new layer. This is performed as follows. The *a priori* probability for a layer of n sites to contain i chain ends when there are a total of m lattice sites and N chain ends in the system is

$$P(i) = \binom{N}{i} (n/m)^i \, (1-n/m)^{N-i}. \tag{27}$$

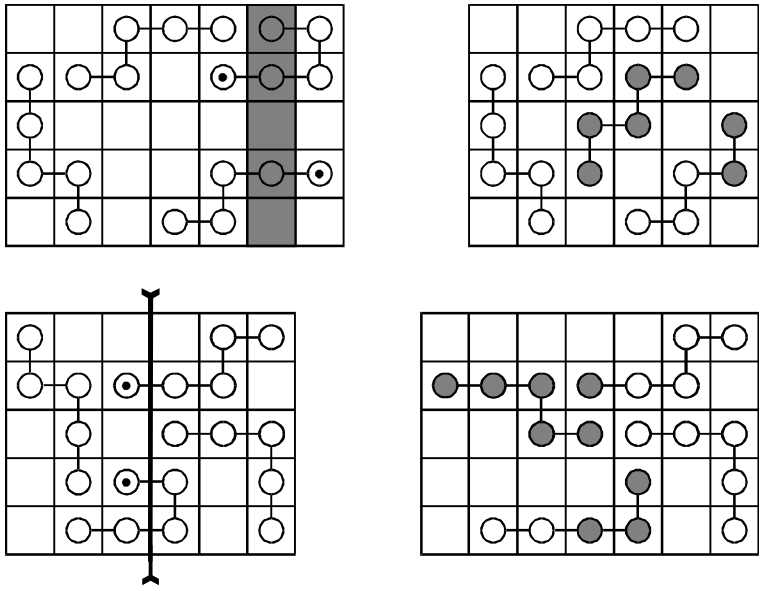

Figure 8. Schematic diagram of volume change steps for constant-pressure lattice simulations. Upper half: lattice contraction; lower half: lattice expansion. Shaded parts of chains have been grown using configurational-biased insertions.

The number of chains to be completely removed and reinserted with one end in the newly created layer is selected from a probability distribution according to equation 27. The chains selected are then removed from the system and the Rosenbluth weight of the old configuration calculated. When all chains cut by the plane of insertion and the extra chains to be completely removed from the system have been taken into account, a new lattice layer is added at the insertion plane. Chains that have been removed completely from the system are regrown with one end on the new inserted layer and cut chains are regrown to their original length using the standard Rosenbluth growth procedure. The step is accepted with probability given in equation 26.

2.4.5. Gibbs-Duhem Integration

While the Gibbs ensemble technique can be used to obtain the densities and compositions of two coexisting phases at one temperature from a single simulation, it relies on insertions of particles to equalize the chemical potentials, and therefore experiences difficulties for dense or highly structured phases. For one-component systems, if a single point on the coexistence curve is known (e.g. from Gibbs ensemble simulations), the remarkably simple and novel method of Kofke [38 ,39] enables the calculation of the complete phase diagram from a series of constant-pressure simulations that do not involve any transfers of particles. While Gibbs-Duhem integration is not, in a

strict sense, a "Gibbs ensemble" method, the complementary nature of the two techniques and some common features (e.g., the use of two-region simulations) justify discussion of Gibbs-Duhem integation in this chapter.

For one-component systems, the method is based on integrating the Clausius-Clapeyron equation over temperature.

$$\left(\frac{dP}{d\beta}\right)_{sat} = -\frac{\Delta H}{\beta \Delta V} \tag{28}$$

where *"sat"* implies that the equation holds on the saturation line, and ΔH is the difference in enthalpy between the two coexisting phases. The right-hand side of equation 28 involves only "mechanical" quantities that can be simply determined in the course of standard Monte Carlo or molecular dynamics simulations. From the known point on the coexistence curve, a change in temperature is chosen, and the saturation temperature at the new temperature is "predicted" from equation 28. Two independent simulations for the corresponding phases are performed at the new temperature, with gradual changes of the pressure as the simulations proceed to take into account the enthalpies and densities at the new temperature as they are being calculated.

Questions related propagation of errors and numerical stability of the method have been addressed in [39] and [40]. Errors in initial conditions resulting from uncertainties in the coexistence densities can propagate and increase with distance from the starting point when the integration path is towards the critical point [40]. Near critical points, the method suffers from instability of a different nature. Because of the small free energy barrier for conversion of one phase into the other, even if the coexistence pressure is set properly, the identity of each phase is hard to maintain and large fluctuations in density are likely. The solution to this last problem is to borrow an idea from the Gibbs ensemble and couple the volume changes of the two regions [39].

Extensions of the method to multicomponent systems are presented in [40]. Two possibilities exist in the case of binary mixtures. In the "osmotic" implementation, simulations are performed at constant temperature, pressure and fugacity of one of the components and the integration is performed with respect to the fugacity of that component. The equation corresponding to equation 28 is

$$\left(\frac{\partial P}{\partial f^A}\right)_{\beta,sat} = \frac{x_I^B / \phi_{II}^A - x_{II}^B / \phi_I^A}{x_I^B Z_{II} - x_{II}^B Z_I} \tag{29}$$

where f^j is the fugacity of component j, x_i^j is the mole fraction of component j in phase i, ϕ_i^j is the fugacity coefficient ($\phi^j P x^j = f^j$) and Z_i is the compressibility factor, PV/kT, of phase i.

In the "semigrand" implementation, simulations are performed in the isothermal semigrand ensemble for which temperature, pressure and the fugacity fraction

($\xi^A = f^A/(f^A + f^B)$ [41] are held fixed and the integration is performed with respect to the fugacity fraction according to

$$\left(\frac{\partial \ln P}{\partial \xi^A}\right)_{\beta,sat} = \frac{x_{II}^A - x_I^A}{\xi^A \xi^B (Z_{II} - Z_I)} \tag{30}$$

A key difference for this case with respect to the case of one-component systems is that it is no longer possible to avoid some form of particle insertions. Species identity changes are required in the semigrand implementation and particle insertions of one of the components are required in the osmotic implementation.

3. Applications

3.1. Simple Fluids and Mixtures

3.1.1. The Truncated Lennard-Jones Potential in Two and Three Dimensions

Although the phase behavior of the Lennard-Jones potential has been extensively studied by many different simulation methods, there is still some uncertainty with respect to the precise location of the critical point. In [15], a systematic study was undertaken of the phase behavior close to the critical point of the Lennard-Jones potential in two and three dimensions truncated at reduced distance r_c^* from 2 to 5. Gibbs ensemble simulations were performed on systems of controlled linear size, and the results were analyzed according to the principles outlined in section 2.2.

The resulting critical temperatures are compared with available literature data in Tables 1 and 2. Wilding and Bruce [45] have obtained accurate estimates of the critical parameters of the two-dimensional Lennard-Jones fluid with r_c^*=2 using finite-size scaling techniques and extremely long grand canonical Monte Carlo simulations. The results are in good agreement with the estimates of [15]. Also in good agreement are the results of [15] and those of Rovere *et al.* for r_c^*=2.5 who used a finite-size scaling analysis of subsystem-block-density distributions. There are no directly comparable data for r_c^*=5, but there are two sets of literature results for the "full" potential. The estimate of Singh *et al* [43] is too low. Following a suggestion of Wilding and Bruce [45], an estimate of the critical temperature for the r_c^*=5 was obtained by assuming that the *ratio* of critical temperatures to the Boyle temperature of the corresponding fluid is approximately constant. The Boyle temperature of the "full" potential is only 0.3% higher than the one with r_c^*=5, which suggests that the difference between the estimate of Smit and Frenkel [42] and of Panagiotopoulos [15] is too high by an order of magnitude to be explained by the different cutoff. Since for finite size systems phase coexistence can be observed at temperatures higher than the infinite-system critical point, this may explain why the result of Smit and Frenkel is higher than the estimates of [15].

TABLE 1. Critical properties of two-dimensional Lennard-Jones fluids

r_c^*	T_C^*	ρ_C^*	Source
none	0.515 ± 0.002	0.355 ± 0.003	Smit and Frenkel [42]
none	0.472	0.33 ± 0.02	Singh *et al.* [43]
5	0.513		Extrapolated from Smit and Frenkel [42]
5	0.497 ± 0.003	0.38 ± 0.01	Panagiotopoulos [15]
2.5	0.472 ± 0.010	0.35 ± 0.01	Rovere *et al.* [44]
2.5	0.477 ± 0.003	0.38 ± 0.02	Panagiotopoulos [15]
2	0.44 ± 0.005	0.368 ± 0.003	Wilding and Bruce [45]
2	0.446 ± 0.003	0.37 ± 0.01	Panagiotopoulos [15]

Results for the three dimensional systems are shown in Table 2. Comparisons of the results with literature data is complicated by the fact that most previous literature studies were for the full [1,8] or the cut-and-shifted potentials [46], not for the truncated potential. If the assumption is made that the ratio of the critical to the Boyle temperatures of each fluid is the same for all fluids (a reasonable assumption based on the calculated critical temperatures), then we can perform the following approximate comparisons. From Smit *et al.*'s estimate [8] of T_c^*=1.316 for the full potential we obtain an extrapolated value T_c^*=1.300 for the potential cut at r_c^*=5. This estimate is somewhat higher than the one of [15], but the difference is just outside the combined simulation uncertainties. In even better agreement with [15] would be an extrapolation of the data of Lotfi *et al.* [2]. From Smit's estimate [46] of T_c^*=1.085 for the cut and shifted potential at r_c^*=2.5 we obtain T_c^*=1.201 for potential cut at r_c^*=2.5, which is also close to but higher than the estimate of [15]. The extrapolation procedure itself may be partly to blame for the differences and it seems justified to clarify whether this small discrepancy can be resolved by detailed calculations with controlled linear system sizes.

TABLE 2. Critical properties of three-dimensional Lennard-Jones fluids

r_c^*	T_C^*	ρ_C^*	Source
none	1.316 ± 0.003	0.304 ± 0.006	Smit and Frenkel [46]
none	1.310	0.314	Lotfi *et al.* [2]
5	1.281 ± 0.005	0.32 ± 0.01	Panagiotopoulos [15]
2.5	1.176 ± 0.008	0.33 ± 0.01	Panagiotopoulos [15]
2	1.061 ± 0.005	0.32 ± 0.01	Panagiotopoulos [15]

3.1.2. Lennard-Jones Mixtures and Applicability of van der Waals 1-fluid Theory

Mixtures of spherical particles of unequal sizes and energetic interactions often arise even in the study of complex liquids, for example in colloidal systems and micellar aggregates. It is of some interest to review the findings of several studies in the recent past on the phase behavior of such systems and the ability of a simple liquid theory, van der Waals 1-fluid theory, to represent their behavior. Harismiadis *et al.* [47] have performed studies of phase equilibria for binary Lennard-Jones mixtures with size parameter ratios between 1 and 2, and energy parameter ratios also between 1 and 2. Unlike-pair parameters were given by the Lorentz-Berthelot rules. For all cases studied, Harismiadis *et al.* found excellent agreement between simulation and theoretical predictions when the Lennard-Jones equation of state of Nicolas *et al.* [48] was used to provide the pure fluid data. The agreement is even better when an improved version of the equation of state is used [49].

Georgoulaki *et al.* [50] have extended the range of asymmetries to 4:1 for both energy and size parameter ratios, and have also examined the behavior of mixtures deviating from the Lorentz-Berthelot rules (ξ_{ij} or ζ_{ij} different from unity). Good agreement was again obtained for the pressure-composition and density-pressure diagrams for highly asymmetric systems with unlike-pair interactions that follow the Lorentz-Berthelot rules and also mixtures that strongly deviate from the Berthelot rule. By contrast, for systems deviating from the Lorentz rule, performance of the theory was less satisfactory. Finally, ternary systems with Lennard-Jones components have been studied by Panagiotopoulos [51] and Tsang *et al.* [52] A typical result from the study of Tsang *et al.* is shown in figure 9. The conclusion from these studies is that the range of applicability of van der Waals 1-fluid theory in describing the phase behavior of Lennard-Jones mixtures is quite broad. This conclusion is in apparent disagreement with results from earlier calculations [53] which suggested that van der Waals one-fluid theory is accurate only for a narrow range of size ratios. However, the earlier studies focused on excess thermodynamic properties which seem to be more sensitive to theoretical inaccuracies than bulk pressures and chemical potentials.

3.2. WATER AND POLAR LIQUIDS

3.2.1. Water and aqueous solutions

Because of its importance, water has been the subject of a large number of simulation studies, but the phase behavior of models for water is only recently starting to emerge. The first Gibbs ensemble simulation study of such a model was by de Pablo and Prausnitz [54] who used the TIP4P model of Jorgensen *et al.* [55] and covered the range from approx. 100 °C to the critical point. The same model, as well as the older TIPS2 model [56], has been studied at lower temperatures by Cracknell *et al.* [23], using the rotational insertion bias method. The SPC model for water [57] has been studied by Mezei [58] using a cavity-biased Gibbs ensemble technique. In these three studies, spherical truncation of the potential at distances beyond half the box length was performed. Some dependence of the results on system size is expected for polar and ionic systems when spherical truncation is used, because of the fluctuation in density and

number of molecules in each of the two phases. The Ewald summation technique which is less sensitive to system size was used by de Pablo *et al.* [59] to study the SPC model for water .

Results for the coexistence curves of the TIP4P and SPC models for water are compared to experimental data in Figure 10. The SPC model reproduces the dielectric constant of liquid water near ambient conditions much better than the TIP4P model [60], but its phase behavior deviates significantly from experiment, especially at higher temperatures. One possible reason for this is the following [61]. One feature of the SPC model that makes it accurate at ambient conditions is that it has a dipole moment of 2.24 D, higher than the bare dipole moment of water of 1.8 D, in order to incorporate polarizability effects that are important for the high density liquid.

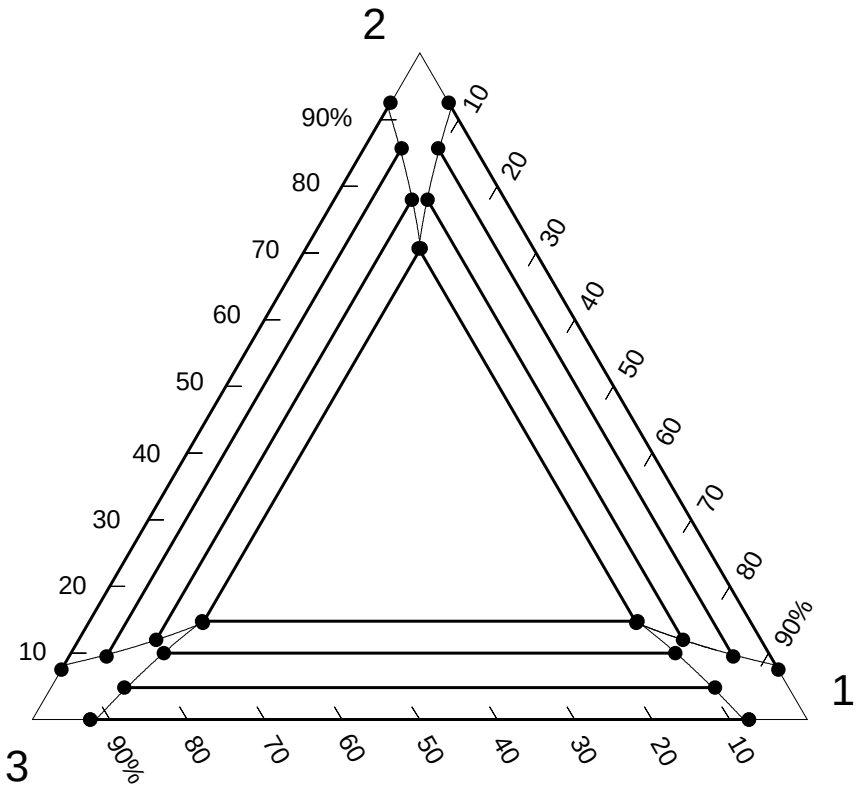

Figure 9. Ternary diagram for a symmetric mixture of Lennard-Jones particles with all pure components identical at T^*= 1, P^*= 2.0. Unlike-pair potential well depth is 75% of the like pair depth, while like and unlike-pair size parameters are equal [52]. Gibbs ensemble simulation results are represented by the thick circles and thick tie lines. Predictions of van der Waals 1-fluid theory are represented by the thin phase envelope.

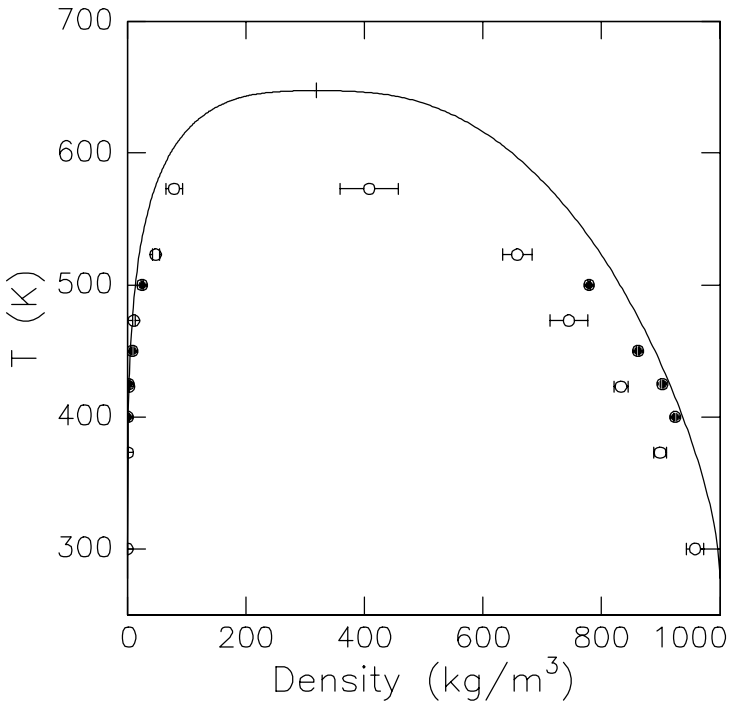

Figure 10. Phase diagrams for SPC (○) and TIP4P (●) models for water [59, 54] compared to experimental results (——, critical point marked by +).

Strauch and Cummings [61] examined the phase behavior of an SPC-like model for which the dipole moment was reduced to 1.8 D in the gas phase. The results were only slightly better than the unmodified SPC model. One conclusion from these studies is that an intermolecular potential model for water that accurately reproduces dielectric properties of the liquid at ambient conditions and the phase behavior at high temperatures is not yet available.

A study of the vapor-liquid phase behavior of binary and ternary mixtures with water, methanol and NaCl are reported in [19]. Good agreement was obtained for the phase envelope of water/methanol mixtures, although in the light of later findings [69] the agreement may be partly fortuitous. For the water/methanol/NaCl ternary system, the qualitatively correct behavior, namely salting out of the methanol, is predicted by the simulations, but the salt effect is overestimated by approximately a factor of 3.

3.2.2. Polar liquids

A number of studies of the phase behavior of polar liquids have appeared in recent years. Phase equilibria of Stockmayer fluids (with Lennard-Jones plus dipole-dipole interactions) with low [62] and high [63] reduced dipole moments have been studied and the results compared to perturbation theories, which deviate significantly from the simulation results for the liquids of high dielectric strengths. Better agreement between perturbation theories and simulation data are found in studies of systems with quadrupole-quadrupole

interactions [64 ,65]. Dipolar diatomic molecules have been studied in [66]. In [66], a recent cluster perturbation theory [67] was found to give generally good agreement with simulation results, except for the liquid density for fluids of larger elongation.

A fascinating observation was made by van Leeuwen and Smit [68] who studied the dipolar with varying dispersive interactions, of the form

$$U_{\lambda,\mu}(\mathbf{r}_{ij},\boldsymbol{\mu}_i,\boldsymbol{\mu}_j) = 4\varepsilon\left[\left(\frac{\sigma}{r_{ij}}\right)^{12} - \lambda\left(\frac{\sigma}{r_{ij}}\right)^{6}\right] + \frac{\mu^2}{r_{ij}^3}\left[\boldsymbol{\mu}_i\cdot\boldsymbol{\mu}_j - \frac{3}{r_{ij}^2}(\boldsymbol{\mu}_i\cdot\mathbf{r}_{ij})(\boldsymbol{\mu}_j\cdot\mathbf{r}_{ij})\right] \qquad (31)$$

where μ is the dipole moment, $\boldsymbol{\mu}_i$ is the orientation of the dipole of particle i, $\mathbf{r}_{ij}$ is the vector connecting the two particles, and λ is a parameter controlling the strength of the dispersive interactions. The critical temperature and density were found to be monotonically decreasing functions of the strength of the dispersive interactions, and no direct phase coexistence could be detected with Gibbs ensemble simulations for values of $\lambda<0.3$. The dipolar liquid at low values of λ and low densities and temperatures was found to have a polymer-like structure. The simulations reported in [68] suggest that a minimum amount of dispersive energy is required to observe a van der Waals-like vapor-liquid curve

A number of studies for realistic potential models of polar liquids have been reported. Of particular interest is the study of van Leeuwen and Smit [69] who tested the predictions of several parameter sets for a unified-atom model of methanol. Predictions of the phase behavior for one of the models were previously made in [58]. Parameters for realistic potential models have been obtained in the past primarily from thermodynamic and structural data of liquids at ambient conditions. When tested against experimental data over a wide range of temperatures and densities such parameters are unlikely to result in satisfactory predictions. In [69], a new parameter set was obtained that predicts phase coexistence properties over a wide range of conditions.

3.3. IONIC, ASSOCIATING AND REACTING FLUIDS

3.3.1. The Phase Behavior of the Restricted Primitive Model for Ionic Systems

Electrolyte solutions, molten salts, and certain colloidal systems are all examples of systems in which the dominant interparticle forces are coulombic interactions. Coulombic interactions are of infinite range, since the potential decays only with the first power of interionic distance in an unshielded system. Accurate statistical-mechanical descriptions of these systems are difficult to obtain, especially at low temperatures. A class of simple models for ionic systems are charged hard sphere models, a special case of which is the restricted primitive model (charged hard spheres of equal diameter). It has been postulated for quite some time now that charged hard sphere systems exhibit vapor-liquid coexistence [78]. There are, however, significant disagreements among results of previous investigations. Potentially serious shortcomings, such as the use of small systems or special boundary conditions and particle transfer methods, can be identified in many previous simulation studies.

The main obstacle to successful simulations of ionic fluids in the low temperature region where coexistence occurs is the strong association of ions at distances close to contact [70] and the resulting extremely slow equilibration. The biased transfer techniques described in section 2.4.2 have been applied to calculate the phase envelope for the restricted primitive model [24]. The results are shown in Fig. 11 and are in modest agreement with previous results using Gibbs ensemble simulations with single-ion transfers [71], the theoretical work of Fisher and Levin [72] and Gibbs ensemble Monte Carlo results of Caillol [73] obtained on a 4-dimensional hypersphere, except for a relatively minor difference in the predicted critical temperature. This agreement suggests that the coexistence curve for the restricted primitive model is now well established.

3.3.2. Associating and Reacting Fluids

Phase equilibria of simple model associating fluids have been studied in [74] and [28]. The models used in these studies are shown in figure 12. The earlier study [74] was for fluids with relatively weak association bond strengths and used the standard version of the Gibbs ensemble. In [28], stronger association bond strengths are studied, and a version of the Gibbs ensemble to handle strongly associating and reactive systems was developed as described in section 2.4.2. For all association strengths covered, the thermodynamic perturbation theory of Wertheim [75] was found to give an excellent account of the phase behavior and the fraction of monomers in both phases when used in connection with an accurate equation of state for the pure Lennard-Jones fluid [49]. Studies of nitric oxide dimerization were also performed in [28] and the results compared favorably to available experimental data.

3.4. PHASE TRANSITIONS IN CHAIN AND POLYMERIC SYSTEMS

3.4.1. Lattice Models

The phase behavior of lattice polymeric systems is primarily covered in the chapter by Binder. Here, we briefly summarize some recent calculations [36] of phase equilibria for a simple lattice polymeric model using the Gibbs ensemble technique described in section 2.4.3. The model used is a homopolymer version of a model proposed by Larson [76] for the study of block copolymeric systems. Monomeric beads are placed on a simple cubic lattice, but interactions are active and the chain backbone can proceed along all diagonal directions on the lattice. The coordination number for the model is 26, a characteristic of the model that facilitates calculations with the lattice version of the Gibbs ensemble because it allows for more possibilities for chain regrowth on removal and additions of new layers.

The phase diagrams of the model for chain lengths from 8 to 128 are shown in figure 13. Even taking into account that the model has a high coordination number, it is remarkable that chain lengths of 128 can be studied with reasonable sampling efficiency,

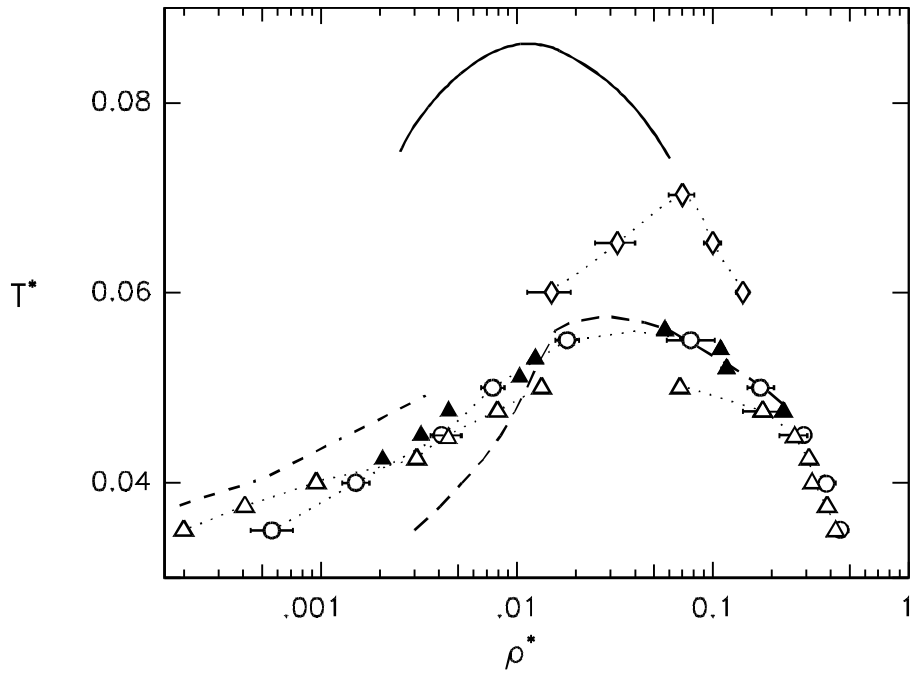

Figure 11. Phase diagram for the restricted primitive model [adapted from 24]. (···Δ···) Gibbs ensemble with biased pair transfers; (···○···) Gibbs ensemble with single ion transfers [71]; (···▲···) Gibbs ensemble on a 4-dimensional hypersphere [73]; (– – –) theory of Fisher and Levin [72]; (– – · – –) lower limit for the vapor density by Gillan [77]; (···◊···) Density scaling Monte Carlo [4]; (—) Stell *et al.* [78]. Dotted lines are arbitrarily drawn through the points for visual clarity.

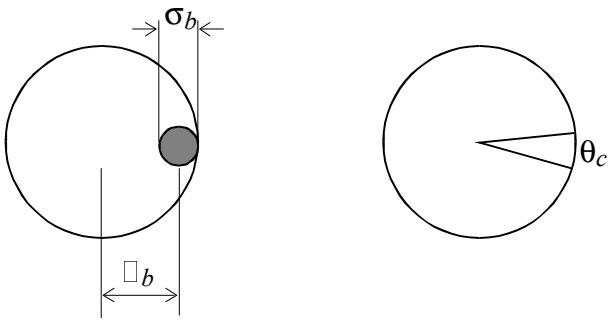

Figure 12. Potentials for model associating fluids. Left: a spherical bonding site of diameter σ_b is placed at a distance r_b from the center of a Lennard-Jones particle. Right: a conical bonding site with a cone angle of θ_c.

given that for the lattice expansion and contraction steps several chains need to be cut and regrown to their original length. The qualitative features of the phase diagram are comparable to experimental data for coexistence curves in polymer/solvent binary mixtures [79] and experimental and simulation results for the coexistence curves at high temperatures for normal alkanes [82]. As also predicted by mean-field theories for polymer solutions such as Flory-Huggins theory [80], the critical temperature increases with chain length and the critical density decreases. Quantitative comparisons of simulation results for the scaling of critical temperature with chain length and the Flory-Huggins and Quggenheim quasi-chemical theories are presented in figure 14. Both mean-field theories overestimate the critical temperatures by about 20%, with the Guggenheim theory being closer to the simulation data. These observations are in qualitative agreement with the findings of Sariban and Binder [81] and Madden *et al.* [30].

3.4.2. Continuous-space models

Simulations of continuous-space models of chain molecules have been performed by a combination of Gibbs ensemble with configurational-bias methods [20,21]. The phase diagram of an 8-mer of Lennard-Jones monomers connected by freely rotating bonds of fixed length σ has been calculated by Mooij *et al.* [20]. The calculations of Laso *et al.* [21] were for a simple model for linear alkanes consisting of "fused" Lennard-Jones beads representing methylene groups connected by rigid bonds at rigid angles. In addition to Lennard-Jones interactions, internal rotations about carbon-carbon bonds were hindered by a torsional potential. Calculations of *n*-pentane to *n*-pentadecane were performed and good agreement with experimental data for the saturated liquid and vapor densities of the corresponding alkanes was obtained.

Perhaps the most spectacular application of the Gibbs ensemble to date in a "predictive" fashion has been provided by the calculation of Siepmann *et al.* [82] of the critical properties of *n*-alkanes. The model used in [82] was a unified-atom model containing non-bonded, bond-bending and angle torsion terms with parameters shown in Table 3.

TABLE 3. Parameters of the *n*-alkane model of Siepmann *et al.* [82]

Physical aspect	Potential function	Parameters
Non-bonded interactions	$U_{LJ}(r_{ji}) = 4\varepsilon_{ij}\left[\left(\frac{\sigma_{ij}}{r_{ij}}\right)^{12} - \left(\frac{\sigma_{ij}}{r_{ij}}\right)^{6}\right]$	$\sigma_{CH_3} = \sigma_{CH_2} = 3.93$ Å $\varepsilon_{CH_3} = 114.0$ K $\varepsilon_{CH_2} = 47.0$ K
Bond-bending	$U_{bending}(\theta_i) = \frac{1}{2} k_\theta (\theta_i - \theta_{eq})^2$	$k_\theta = 62,500$ K rad^{-2} $\theta_{eq} = 114^\circ$
Angle torsion	$U_{torsion}(\phi_i) = a_1(1+\cos\phi_i) + a_2(1-\cos(2\phi_i)) + a_3(1+\cos(3\phi_i))$	$a_1 = 355.03$ K $a_2 = -68.19$ K $a_3 = 791.32$ K

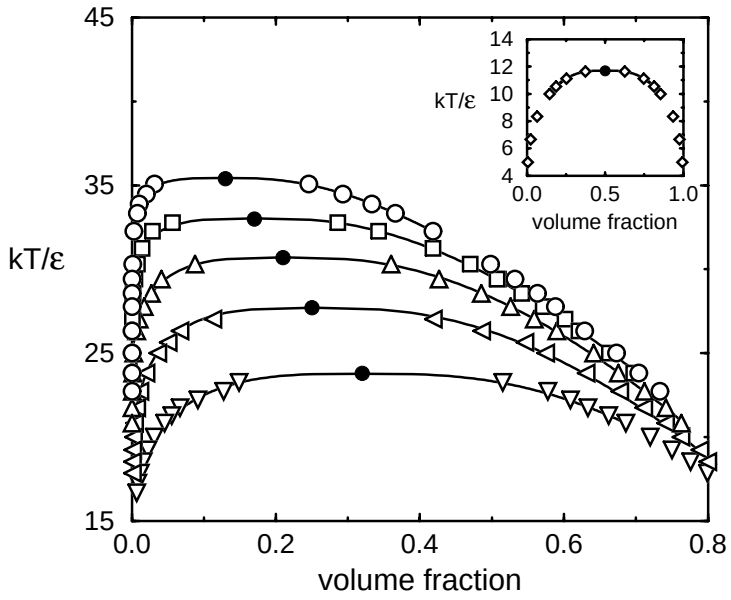

Figure 13. Phase diagram for a cubic lattice homopolymer model of coordination number 26 [36]. Curves from top to bottom are for chain lengths n=128,64,32,16 and 8. Inset shows data for n=1. Curves are fitted using the scaling relationships (equation 13).

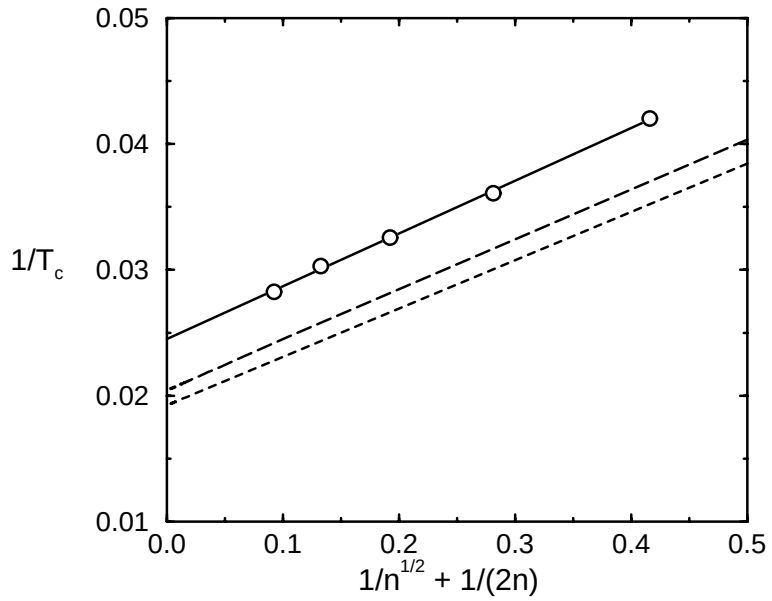

Figure 14. Inverse reduced critical temperatures versus $1/\sqrt{n}+1/(2n)$ where n is the chain length [36]. Points are from simulation and the continuous line is a least-squares fit of the points. (- - -) Flory-Huggins theory (— —) Guggenheim's quasi-chemical theory.

The parameters were obtained by fitting phase coexistence properties and the critical parameters of *n*-octane and the critical points of the hydrocarbons with 16 - 48 carbon atoms were predicted using the potential model. Measurements of critical properties of long-chain alkanes is difficult because of thermal decomposition, but knowledge of these properties is important for developing reliable engineering models for hydrocarbons [83]. There were conflicting experimental measurements and correlations for intermediate-range alkanes, which the simulations of Siepmann *et al.* were able to resolve.

In the present section on calculations of the phase behavior of continuous-space polymeric models, it is worth mentioning a methodology that is complementary to configurational-bias Gibbs ensemble calculations for long chain molecules. The methodology is based on the concept of the incremental chemical potential. For a chain of length n present in infinite dilution in an appropriate medium the incremental chemical potential, $\mu_r^+(x)$, is given by

$$\mu_r^+(n) = -kT \ln\left\langle \exp(-\beta U_{n+1}^+)\right\rangle, \tag{32}$$

where U_{n+1}^+ is the energy experienced during growth of the chain from length n to length n+1. The total chemical potential of a chain of length n can be obtained by summing the incremental chemical potentials of all chains of shorter length,

$$\mu_r^{chain}(l) = \sum_{n=1}^{l} \mu_r^+(n) \ . \tag{33}$$

In principle, l different simulations need to be performed in order to obtain the chain chemical potential of a chain of length l according to Eq. (33). In practice, the chain length dependence of the chemical potential is often found to be weak [84], and a significantly reduced number of simulations is required. This, however, is not the case for the incremental chemical potential of a realistic chain model [85] which was observed to approach an asymptotic value only for significantly longer chains.

The incremental chemical potential concept allows calculations of chemical potential and phase equilibria for chain molecules that are too long to be accessible with Gibbs ensemble calculations even when combined with configurational-bias sampling. A calculation of this type has been reported for a bead-spring polymeric model by Sheng *et al.* [86] for chains length up to 100. Because the bead-spring model has considerably more flexibility than an articulated-atom or unified-atom model, each bead effectively corresponds to several carbon atoms of an alkane chain. The main characteristics of the phase behavior obtained for this model are comparable to the phase behavior of the lattice polymeric model described in section 3.4.1.

4. Summary and Conclusions

The present chapter has reviewed recent progress in the field of simulation of phase transitions using Gibbs ensemble and related methods. The range of applicability of these methods has expanded in recent years from simple Lennard-Jones potentials to polymeric, ionic and reacting systems, primarily by introduction of configurational-bias sampling methods. Issues related to the behavior of Gibbs ensemble simulations at the vicinity of critical points have been clarified and methods have been developed to obtain estimates of critical parameters that are in good agreement with estimates obtained with finite-size scaling techniques. At least for one-component systems, phase boundaries can be determined with a higher accuracy than is possible from Gibbs ensemble simulations using thermodynamic-scaling Monte Carlo methods [4] or by calculations of the chemical potential for a series of state points [2].

The application of any molecular simulation methodology for the purpose of predictions outside the range of availability of experimental data requires the selection of appropriate intermolecular potentials. In the author's view, such potentials are at the moment best to be obtained by fitting parameters of empirical potential forms to experimental data. The study of Siepmann *et al.*, [82] which involved using selected experimental results for low-chain length alkanes to obtain the parameters of an empirical potential and used it to predict the phase behavior of longer-chain alkanes at experimentally inaccessible conditions is a case in point. An open question in this area is whether density-dependent potentials [87] can be used to model the change in importance of three-body forces at liquid densities without sacrificing the simplicity of pair-wise additivity.

Despite the progress described here and elsewhere in methodologies for the molecular simulation of phase coexistence properties of systems of interest for the chemical and materials processing industries, several important classes of systems remain difficult to handle. Solids are one such class. At the moment, the only realistic method for determining the phase behavior of solids is thermodynamic integration (chapter by Frenkel in this volume). A comparable situation exists for highly ordered systems, such as ones forming liquid crystals, and associating systems, such as surfactant solutions that form large micellar aggregates.

5. Acknowledgments

Research work in the author's group described in this chapter has been supported by the Division of Chemical Sciences, Office of Basic Energy Sciences, U.S. Department of Energy and a PYI award from the U.S. National Science Foundation. The author is a Camille and Henry Dreyfus Teacher-Scholar. I would also like to acknowledge the hospitality of NCSR Demokritos in Athens, Greece, during preparation of this manuscript and the lectures on which it is based.

6. References

1 . Panagiotopoulos, A.Z. (1987) Direct determination of phase coexistence properties of fluids by Monte Carlo simulation in a new ensemble, *Molec. Phys.* **61**, 813-826.

2 . Lotfi, A., Vrabec, J., and Fischer, J. (1992) Vapour liquid equilibria of the Lennard-Jones fluid from the NpT plus test particle method, *Molec. Phys.* **76**, 1319-33.

3 . Torrie, G.M. and Valleau, J.P. (1977) Nonphysical sampling distributions in Monte Carlo free-energy estimation: Umbrella sampling, *J. Comp. Phys.* **23**, 187-199.

4 . Valleau, J. P. (1991) Density-scaling: A new Monte Carlo technique in statistical mechanics, *J. Comp. Phys.* **96**, 193-216.

5 . Panagiotopoulos, A.Z. (1992) Direct determination of fluid phase equilibria by simulation in the Gibbs ensemble: A review, *Molec. Simulation* **9**, 1-23.

6 . Panagiotopoulos, A.Z. (1994) Molecular simulation of phase equilibria, chapter in E. Kiran. and J.M.H. Levelt Sengers (eds.), *Supercritical Fluids - Fundamentals for Application*, NATO ASI Series E, Kluwer Academic Publishers: Dordrecht, The Netherlands.

7 . Panagiotopoulos, A.Z., Quirke, N., Stapleton, M. and Tildesley, D.J. (1988) Phase equilibria by simulation in the Gibbs ensemble. Alternative derivation, generalization and application to mixture and membrane equilibria, *Molec. Phys.* **63**, 527-545.

8 . Smit, B., De Smedt, Ph., Frenkel, D. (1989) Computer simulations in the Gibbs ensemble, *Molec. Phys.* **68**, 931-50.

9 . Smit, B., Frenkel, D. (1989) Calculation of the chemical potential in the Gibbs ensemble, *Molec. Phys.* **68**, 951-8.

10 . Smit, B. (1993) Computer simulations in the Gibbs ensemble, in M.P. Allen and D.J. Tildesley (eds), *Computer Simulation in Chemical Physics,* NATO ASI Ser. C: vol. 397, Kluwer Academic Publishers: Dordrecht, The Netherlands.

11 . Panagiotopoulos, A.Z. (1989) Exact Calculations of fluid-phase equilibria by Monte Carlo simulation in a new statistical ensemble, *Int. J. Thermophys.* **10**, 447-457.

12 . Smit, B. (1990) *Simulation of phase coexistence: from atoms t o surfactants*, doctoral dissertation, Univ. of Utrecht, The Netherlands.

13 . Mon, K.K. and Binder, K. (1992) Finite size effects for the simulation of phase coexistence in the Gibbs ensemble near the critical point. *J. Chem. Phys.* **96**, 6989-95.

14 . Recht, J. R. and Panagiotopoulos, A.Z. (1993) Finite-size effects and approach to criticality in Gibbs ensemble simulations. *Molec. Phys.* **80,** 843-852.

15 . Panagiotopoulos, A.Z. (1994) Molecular simulation of phase coexistence: Finite-size effects and determination of critical parameters for two- and three- dimensional Lennard-Jones fluids, accepted for publication, *Int. J. Thermophys.*

16 . Valleau, J. (1994) presentation at the 11th International Symposium on Thermophysical Properties, Boulder, CO.

17 . Panagiotopoulos, A. Z. (1987) Adsorption and capillary condensation of fluids in cylindrical pores by Monte Carlo simulation in the Gibbs ensemble. *Molec. Phys*. **62,** 701-719.

18 . Heffelfinger, G.S., van Swol, F. and Gubbins, K.E. (1987) Liquid-vapor coexistence in a cylindrical pore. *Mol. Phys.*, **61**, 1381-90.

19 . Strauch, H. J. and Cummings, P. T. (1993) Gibbs ensemble simulation of mixed solvent electrolyte solutions, *Fluid Phase Equil.* **83**, 213-22.
20 . Mooij, G.C.A.M., Frenkel, D. and Smit, B. (1992) Direct simulation of phase equilibria of chain molecules. *J. Phys. Condens. Matter* **4**, L255-L259.
21 . Laso, M., de Pablo, J.J. and Suter, U.W. (1992) Simulation of phase equilibria for chain molecules. *J. Chem. Phys.* **97**, 2817-19.
22 . Mooij, G.C.A.M. (1993) *Novel techniques for the study o f polymer phase equilibria* , Ph. D. thesis, Univ. of Utrecht, The Netherlands.
23 . Cracknell, R.F., Nicholson, D., Parsonage, N.G. and Evans, H. (1990) Rotational insertion bias: a novel method for simulating dense phases of structured particles, with particular application to water, *Mol. Phys.*, **71**, 931-943.
24 . Orkoulas, G. and Panagiotopoulos, A.Z. (1994) Free energy and phase equilibria for the restricted primitive model of ionic fluids from Monte Carlo Simulations, *J. Chem. Phys.,* **101**, 1452-59.
25 . Theodorou, D.N. and Suter, U.W. (1985) Geometrical considerations in model systems with periodic boundaries, *J. Chem. Phys.* **82**, 955-66.
26 . Tsangaris, D.M and de Pablo, J.J. (1994) Bond-bias simulation of phase equilibria for strongly associating fluids. *J. Chem. Phys.*, **101,** 1477.
27 . Shaw, M.S. (1991) Monte Carlo simulation of equilibrium chemical composition of molecular fluid mixtures in the $N_{atoms}PT$ ensemble, *J. Chem. Phys.* **94**, 7550-4.
28 . Johnson, J.K., Panagiotopoulos, A.Z. and Gubbins, K.E. (1994) Reactive canonical Monte Carlo. A new simulation technique for reacting or associating fluids, *Molec. Phys.*, **81**, 717-733.
29 . Smith, W. R. and Triska, B. (1994) The reaction ensemble method for the computer simulation of chemical and phase equilibria. I. Theory and basic examples, *J. Chem. Phys.* **100**, 3019-27.
30 . Madden, W.G., Pesci, A.I. and Freed, K.F. (1990). Phase equilibria of lattice polymer and solvent: tests of theories against simulations. *Macromolecules* **23**, 1181-91.
31 . Sariban, A.; Binder, K. (1987). Critical properties of the Flory-Huggins lattice model of polymer mixtures. *J. Chem. Phys.* **86**, 5859-73.
32 . Deutsch, H.P. and Binder, K. (1993). The mean field to Ising crossover in the critical behavior of polymer mixtures: a finite size scaling analysis of Monte Carlo simulations. *J. Phys. II France* **3**, 1049-73.
33 . Deutsch, H.P. and Binder, K. (1993). Simulation of first- and second- order transitions in asymmetric polymer mixtures. *Makromoleculare Chemie-Macromolecular Symposia* , **65**, 59-68.
34 . Gauger, A.; Pakula, T. (1993). Phase equilibrium in mixtures of flexible and stiff polymers studied by Monte Carlo simulation. *J. Chem. Phys.* **98**, 3548-3553.
35 . Mackie, A.D.; Panagiotopoulos, A.Z.; Kumar, S.K. and Frenkel, D. (1994) *Europhys. Letts*., in press.
36 . Mackie, A.D.; Panagiotopoulos, A.Z. and Kumar, S.K. (1994) submitted for publication, *J. Chem. Phys*.
37 . Rosenbluth, M.N.; Rosenbluth, A.W. (1955). Monte Carlo calculations of the average extension of molecular chains. *J. Chem. Phys.* **23**, 356-9.

38 . Kofke, D.A. (1993) Gibbs-Duhem integration: A new method for direct evaluation of phase coexistence by molecular simulation, *Molec. Phys.* **78**, 1331-6.
39 . Kofke, D.A. (1993) Direct evaluation of phase coexistence by molecular simulation via integration along the saturation line, *J. Chem. Phys.* **98**, 4149-4162.
40 . Mehta, M. and Kofke, D.A. (1994) Coexistence diagrams of mixtures by molecular simulation, *Chem. Eng. Sci.*, in press.
41 . Kofke, D. A, Glandt, E. D. (1988) Monte Carlo simulation of multicomponent equilibria in a semigrand canonical ensemble, *Molec. Phys.* **64**, 1105-31.
42 . Smit, B., Frenkel, D. (1991) Vapor-liquid equilibria for the two-dimensional Lennard-Jones fluid(s), *J. Chem. Phys.* **94**, 5663-8.
43 . Singh, R.R., Pitzer, K.S., de Pablo, J.J. and Prausnitz, J.M. (1990) Monte Carlo Simulation of phase equilibria for the two-dimensional Lennard-Jones fluid in the Gibbs ensemble, *J. Chem. Phys.* **92**, 5463-6.
44 . Rovere, M., Nielaba, P., Binder, K. (1993) Simulation studies of gas-liquid transitions in two dimensions via a subsystem-block-density distribution analysis, *Z. Phys.* **90**, 215-228.
45 . Wilding, N.B. and Bruce, A.D. (1992) Density fluctuations and field mixing in the critical fluid, *J. Phys.: Condens. Matter* **4**, 3087-3108; Bruce, A.D. and Wilding, N.B. (1992) Scaling fields and universality of the liquid-gas critical point, *Phys. Rev. Lett.* **68**, 193-6.
46 . Smit, B. (1992) Phase diagrams of Lennard-Jones fluids, *J. Chem. Phys.* **96,** 8639-8640.
47 . Harismiadis, V. I., Koutras, N. K., Tassios. D. P., Panagiotopoulos, A. Z. (1991) How good is conformal solutions theory for phase equilibrium predictions? Gibbs ensemble simulations of binary Lennard-Jones mixtures, *Fluid Phase Equil*. **65**, 1-18.
48 . Nicolas, J.J., Gubbins, K.E., Streett, W.B., Tildesley, D.J. (1979) Equation of state for the Lennard-Jones fluid, *Molec. Phys.* **37**, 1429-54.
49 . Johnson, J. K., Zollweg, J. A., Gubbins, K. E. (1993) The Lennard-Jones equation of state revisited, *Molec. Phys.* **78**, 591-618.
50 . Georgoulaki, A.M., Ntouros, I.V., Tassios D.P. and Panagiotopoulos, A.Z. (1994) Phase equilibria of binary Lennard-Jones mixtures: Simulation and van der Waals 1-fluid theory, accepted for publication, *Fluid Phase Equil.*, 1994.
51 . Panagiotopoulos, A.Z. (1989) Gibbs-ensemble Monte Carlo simulations of phase equilibria in supercritical fluid systems, in K.P. Johnston and J. Penninger (eds.) "Supercritical Fluid Science and Technology," *ACS Symposium Ser.*, **406**, 39-51.
52 . Tsang, P.C., White, O.N., Perigard, B.Y., Vega L.F. and Panagiotopoulos, A.Z. Phase equilibria in ternary Lennard-Jones systems, submitted for publication, *Fluid Phase Equil.,* 1994.
53 . Singer, J.V.L. and Singer, K. (1972) Monte Carlo calculation of thermodynamic properties of binary mixtures of Lennard-Jones (12-6) liquids. *Molec. Phys.* **24**, 357-90.
54 . De Pablo, J.J. and Prausnitz, J.M. (1989) Phase equilibria for fluid mixtures from Monte Carlo simulation, *Fluid Phase Equil.* **53**, 177-89.
55 . Jorgensen, W.L., Chandrasekhar, J. and Madura, J.D. (1983) Comparison of simple potential functions for simulating liquid water, *J. Chem. Phys.* **79**, 926-35.
56 . Jorgensen, W.L. (1982) Revised TIPS for simulations of liquid water and aqueous solutions, *J. Chem. Phys.* **77**, 4156-63.
57 . Berendsen, H.J.C., Postma, J.M.P., van Gusteren W.F. and Hermans, J., in Pullman, B. (ed.) *Intermolecular Forces*, Jerusalem Symp. Quantum Chem. Biochem. **14**, 331 (1981).

58 . Mezei, M. (1992) Theoretical Calculation of the Liquid-Vapor Coexistence Curve of Water, Chloroform and Methanol with the Cavity-Biased Monte Carlo Method in the Gibbs Ensemble, *Molec. Simulation* **9**, 257-267.
59 . De Pablo, J.J., Prausnitz, J.M., Strauch, H.J. and Cummings, P.T. (1990) Molecular Simulation of water along the liquid-vapor coexistence curve from 25° C to the critical point, *J. Chem. Phys.* **93**, 7355-9.
60 . Strauch, H.J. and Cummings, P.T. (1989) Computer simulation of the dielectric properties of liquid water, *Molec. Simulation* **2**, 89-104.
61 . Strauch, H.J., Cummings, P.T. (1992) Comment on: Molecular simulation of water along the liquid-vapor coexistence curve from 25° C to the critical point, *J. Chem. Phys.* **96**, 864-5.
62 . Smit, B., Williams, C.P., Hendriks, E.M. and de Leeuw, S.W. (1989) Vapour-liquid equilibria for Stockmayer fluids, *Molec. Phys.* **68**, 765-9.
63 . Van Leeuwen, M. E., Smit, B., Hendriks, E. M. (1993) Vapour-liquid equilibria of Stockmayer fluids. Computer simulations and perturbation theory, *Molec. Phys.* **78**, 271-83.
64 . Smit, B., Williams, C.P. (1990) Vapour-liquid equilibria for quadrupolar Lennard-Jones fluids, *J. Phys.: Condensed Matter* **2**, 4281-88.
65 . Stapleton, M.R., Tildesley, D.J., Panagiotopoulos, A.Z., Quirke, N. (1989) Phase equilibria of quadrupolar fluids by simulation in the Gibbs ensemble, *Molec. Simulation* **2**, 147-62.
66 . Dubey, G.S., O'Shea, S.F. and Monson, P.A. (1993) Vapour-liquid equilibria for two-center Lennard-Jones diatomics and dipolar diatomics, *Molec. Phys.* **80**, 997-1007.
67 . Lupkowski, M. and Monson, P.A. (1989) *Molec. Phys.*, **67**, 53.
68 . Van Leeuwen, M.E., Smit, B. (1993) What makes a polar liquid a liquid?, *Phys. Rev. Lett.* **71**, 3991-4.
69 . Van Leeuwen, M.E. and Smit, B. (1994) Molecular simulation of the vapor-liquid coexistence curve of methanol, preprint.
70 . Hafskjold, B. and Stell, G. (1982) The equilibrium statistical mechanics of simple ionic liquids in E.W. Montroll and J.L. Lebowitz (eds.) *The Liquid State o f Matter: Fluids, Simple and Complex*, North-Holland, pp. 175-274.
71 . Panagiotopoulos, A.Z. (1992) Molecular simulation of phase equilibria: simple, ionic and polymeric fluids, *Fluid Phase Equil.* **76**, 97-112.
72 . Fisher, M.E., Levin, Y. (1993) Criticality in ionic fluids: Debye-Hückel, Bjerrum, and beyond, *Phys. Rev. Lett.* **71**, 3826-9.
73 . Caillol, J. M. (1994) A Monte Carlo study of the liquid-vapour coexistence of charged hard spheres, *J. Chem. Phys.* **100**, 2161-69.
74 . Johnson, J.K., Gubbins, K.E. (1992) Phase equilibria for associating Lennard-Jones fluids from theory and simulation, *Molec. Phys.* **77**, 1033-1053.
75 . Wertheim, M.S. (1986) *J. Stat. Phys.* **42**, 477.
76 . Larson, R.G., Scriven, L.E. and Davis, H.T. (1985) Monte Carlo simulation of amphiphile-oil-water systems, *J. Chem. Phys.* **83**, 2411-20.
77 . Gillan, M.J. (1983) Liquid-vapour equilibrium in the restricted primitive model for ionic liquids, *Molec. Phys.* **49**, 421-442.

78 . Stell, G., Wu, K.C., Larsen, B. (1976) Critical point in a fluid of charged hard spheres, *Phys. Rev. Lett.* **37**, 1369-72.
79 . Dobashi, T., Nakata, M. and Kaneko, M. (1980) Coexistence curve in polystyrene in methylcyclohexane. I. Range of simple scaling and critical exponents, *J. Chem. Phys.* **72**, 6685-91.
80 . Flory, P.J. (1953) *Principles of Polymer Chemistry*, Cornell University Press, Ithaca, New York.
81 . Sariban, A., Binder, K. (1987) Critical properties of the Flory-Huggins lattice model of polymer mixtures, *J. Chem. Phys.* **86**, 5859-73.
82 . Siepmann, J.I., Karaborni, S., Smit, B. (1993) Simulating the critical behavior of complex fluids, *Nature* **365**, 330-2.
83 . Tsonopoulos, C.; Tan, Z. (1993) The critical constants of normal alkanes from methane to polyethylene II. Application of the Flory Theory, *Fluid Phase Equilib.* **83**, 127.
84 . Szleifer, I., Panagiotopoulos, A.Z. (1992) Chain length and density dependence of the chemical potential of lattice polymers, *J. Chem. Phys.* **97**, 6666-73.
85 . De Pablo, J.J., Laso, M. and Suter, U.W. (1992) Estimation of the chemical potential of chain molecules by simulation, *J. Chem. Phys.* **96**, 6157-62.
86 . Sheng, Y.-J., Panagiotopoulos, A. Z., Kumar, S. K., Szleifer, I. (1994) Monte Carlo simulation of phase equilibria for a bead-spring polymeric model, *Macromolecules* **27**, 400-6.
87 . Smit, B., Hauschild, T., Prausnitz, J.M. (1992) Effect of a density-dependent potential on the phase behavior of fluids, *Molec. Phys.* **77**, 1021-1031.